International Journal of Heat and Mass Transfer 52 (2009) 2161–2165

Contents lists available at ScienceDirect

International Journal of Heat and Mass Transfer

journal homepage: www.elsevier.com/locate/ijhmt

Technical Note

Matrix free meshless method for transient heat conduction problems

Xiao Hua Zhang, Jie Ouyang *, Lin Zhang

Department of Applied Mathematics, Northwestern Polytechnical University, Xi'an 710072, China

A R T I C L E I N F O

Article history:
Received 30 January 2008
Received in revised form 12 November 2008
Available online 29 December 2008

Keywords:
Meshless method
EFGM
Heat conduction
Matrix free

A B S T R A C T

In the paper, the element free Galerkin method (EFGM) is applied to calculate two-dimensional unsteady state heat conduction problems. As is well known, most of the meshless methods have higher computational cost than that of finite element method (FEM). In order to overcome this shortcoming especially for transient heat conduction problems, mass lumping procedure is adopted in EFGM, which can decrease the computational cost evidently. Moreover, this technique which can simplify the solution procedure makes the essential boundary conditions enforced directly. The results obtained by EFGM combining mass lumping technique are compared with those obtained by finite element method as well as analytical solutions, which shows that the solutions of the present method are in good agreement with FEM's and analytical solutions.

1. Introduction

Many practical heat transfer applications are unsteady (transient) in nature and in such problems the temperature varies with respect to time. For example, in a lot of components of industrial plants such as boilers, refrigeration and air-conditioning equipment, the heat transfer process is transient during the initial stages of operation. Therefore, the analysis of transient heat conduction is very important. Although analytical techniques such as variable separation can be employed to solve transient heat conduction problems, the solution for practical heat transfer problems by these methods is difficult. As a result, various numerical models have been developed for analyzing transient heat conduction problems. It is noted that numerical methods such as finite element method (FEM), finite volume method (FVM) and finite difference method (FDM) have been well established over the past a few decades and successfully applied to transient heat conduction problems.

Among the methods mentioned above, the spatial domain where the partial differential governing equations are defined is often discretized into meshes. Generally speaking, the creation of suitable meshes is very essential for acquiring accurate results. However, mesh generation process consumes a lot of time and labor for some problems especially for discontinuous, high gradient and 3D problems. The root of these difficulties is the use of mesh in the formulation stage. An attractive option for such problems is the meshless discretization or a finite point discretization approach, which has been popular in recent years. Meshless methods only use a set of nodes scattered within the problem domain as well as a set of nodes scattered on the boundary. Therefore, compared with FEM, meshless methods are well-suited for certain class of problems such as crack propagation, free surface boundaries, dynamic impact problems, phase transformation, larger deformations, discontinuous problems, nonlinear thermal analysis and so on. To date, there exist many meshless methods such as smoothed particle hydrodynamics (SPH) [1], element free Galerkin (EFG) method [1,2], meshless local Petrov–Galerkin (MLPG) method [2], reproducing kernel particle method (RKPM) [1], radial point interpolation method (RPIM) [2] and so on. The more details of these meshless methods can refer to [2]. As a matter of fact, some researchers have applied meshless methods to heat transfer problems. Singh et al. applied EFGM to solve composite heat transfer problems [3,4], unsteady state heat transfer in semi-infinite solid [5] and unsteady nonlinear heat transfer problems [6]. Liu [7] solved the radiative transfer problem by MLPG. Wang et al. [8] developed a meshless numerical model for analyzing transient heat conduction in non-homogeneous functionally graded materials (FGM). Sladek et al. [9,10] used MLPG to analysis transient heat conduction with continuously inhomogeneous and anisotropic FGM, too. Zhang and Ouyang [11] also used the EFGM to analysis the heat transfer due to viscous dissipation in polymer flow. Wu and Tao [12] applied MLPG to compute steady state heat conduction problems of irregular complex domain in 2D domain. Zhang et al. [13] applied SPH to simulate the droplet spreading, splashing and solidification. Among all the meshless methods, the EFGM has become quite popular due to its successful applicability in various fields of engineering [1,2]. So in the paper, we choose EFGM to solve the unsteady state heat conduction problems.

Although meshless methods have a lot of advantages over FEM, as a coin has two sides, they also have some disadvantages. For example, most of the meshless methods (e.g. EFGM) have high computational cost as compared to FEM, especially for transient

* Corresponding author. Tel.: +86 029 8849 5234; fax: +86 029 8849 1000.
E-mail address: jieouyang@nwpu.edu.cn (J. Ouyang).

0017-9310/$ - see front matter © 2008 Elsevier Ltd. All rights reserved.
doi:10.1016/j.ijheatmasstransfer.2008.11.010

Nomenclature

$a_j(\boldsymbol{x})$	non-constant coefficients	T	temperature of the material
c_p	specific heat of the material	T_a	atmospheric temperature
G	heat generation per unit volume	T_{side}	the temperature at the sides except top side
h	heat transfer coefficient	T_{top}	the temperature at the top side
H	the height of the plate	u^h	moving least square approximation
m	number of terms in the basis	$w(\boldsymbol{x}-\boldsymbol{x}_I)$	weight function
N	number of nodes in the domain of influence	W	the width of the plate
n_x, n_y	outward normal to the surface	$\boldsymbol{x}_Q$	Gauss quadrature point
$\boldsymbol{N}(\boldsymbol{x})$	shape functions	ρ	density of the material
$\boldsymbol{P}(\boldsymbol{x})$	complete polynomial basis	Δt	time step
q	boundary heat flux	σ_{ij}	Kronecker delta function

problems. As a matter of fact, if transient problems are solved in an explicit mode, all the transient terms usually lead to mass matrices after spatial and temporal discretizations. Moreover, the band width of these mass matrices obtained by EFGM is usually larger than that obtained by FEM. Therefore, more computational time is needed to solve linear equations. The main object of the paper is to reduce the computational cost of EFGM as much as possible. In FEM, mass lumping procedure is quite prevalent, which can simplify the solution procedure and save much computational time. Thus, we introduce the mass lumping technique to the meshless methods (e.g. EFGM). So far the utilization of this technique combining EFGM has not found in literatures.

The paper is organized into following sections. In Section 2, the details of the EFGM are presented. Section 3 describes the temporal and spatial discretization for the transient equations and matrix lumping technique in detail. The results of numerical example and discussion are presented in Section 4. Finally, Section 5 draws some conclusions on the presented analysis.

2. Review of element free Galerkin method

In the EFGM, the field variable $u(\boldsymbol{x}, t)$ is approximated by moving least squares (MLS) approximation which was initially introduced for data fitting and surface construction in 1981 [1]. The MLS approximation $u^h(\boldsymbol{x}, t)$ of $u(\boldsymbol{x}, t)$ can be defined by [1,2]

$$u^h(\boldsymbol{x},t) = \sum_{j=1}^{m} p_j(\boldsymbol{x}) a_j(\boldsymbol{x},t) = \boldsymbol{P}^{\mathrm{T}}(\boldsymbol{x})\boldsymbol{a}(\boldsymbol{x},t) \tag{1}$$

where $\boldsymbol{P}(\boldsymbol{x})$ is a complete polynomial basis of order m and $\boldsymbol{a}(\boldsymbol{x}, t)$ is coefficient (to be determined) which is the function of the space coordinate $\boldsymbol{x}$ and time t. For the sake of simplicity, linear basis is chosen in the paper.

The unknown coefficient $\boldsymbol{a}(\boldsymbol{x}, t)$ in Eq. (1) is obtained at any point $\boldsymbol{x}$ by minimizing the following weighted, discrete error norm

$$\boldsymbol{J} = \sum_{i=1}^{n} w(\boldsymbol{x}-\boldsymbol{x}_I)\left[u_I(t) - \boldsymbol{P}^{\mathrm{T}}(\boldsymbol{x}_I)\boldsymbol{a}(\boldsymbol{x},t)\right]^2 \tag{2}$$

where $w(\boldsymbol{x}-\boldsymbol{x}_I)$ is a weight function of compact support (often called the domain of influence of node I) and n is the number of nodes whose support includes point $\boldsymbol{x}$. $u_I(t)$ is the parameter associated with node I of the approximation field. The choice of the weight function is more or less arbitrary in practice, and spline function [2] is chosen as weight function in the paper.

Minimization of Eq. (2) with respect to $\boldsymbol{a}(\boldsymbol{x}, t)$ then yields to the following system of linear equations for the coefficient $\boldsymbol{a}(\boldsymbol{x}, t)$:

$$\boldsymbol{A}(\boldsymbol{x})\boldsymbol{a}(\boldsymbol{x}) = \boldsymbol{B}(\boldsymbol{x})\boldsymbol{u}(t) \tag{3}$$

where $\boldsymbol{A}(\boldsymbol{x})$ and $\boldsymbol{B}(\boldsymbol{x})$ can easily be obtained from Eq. (1), and $\boldsymbol{u}(t)$ is the vector of nodal unknowns. If $\boldsymbol{A}$ is invertible, the coefficient $\boldsymbol{a}(\boldsymbol{x}, t)$ can be expressed as

$$\boldsymbol{a}(\boldsymbol{x},t) = \boldsymbol{A}^{-1}(\boldsymbol{x})\boldsymbol{B}(\boldsymbol{x})\boldsymbol{u}(t) \tag{4}$$

Substituting the above equation back into Eq. (1) leads to

$$u^h(\boldsymbol{x},t) = \boldsymbol{P}^{\mathrm{T}}(\boldsymbol{x})\boldsymbol{A}^{-1}(\boldsymbol{x})\boldsymbol{B}(\boldsymbol{x})\boldsymbol{u}(t) = \boldsymbol{N}^{\mathrm{T}}(\boldsymbol{x},t)\boldsymbol{u}(t) \tag{5}$$

where $\boldsymbol{N}(\boldsymbol{x}, t)$ is the vector of MLS shape functions.

The MLS approximation is obtained by a special least squares method, thus the functions obtained by the MLS approximation are smooth curve and they do not pass through the nodal values. Therefore, the MLS shape functions do not, in general, satisfy the Kronecker delta condition at each node, i.e. $N_I(\boldsymbol{x}_J) \neq \delta_{IJ}$. Consequently, the imposition of essential boundary conditions is more complicated than that for the standard FEM. Several methods have been proposed, including Lagrange multipliers [1,2], penalty methods [2], coupled FEM method [1], direct collocation method [1,2] and so on. In the paper, direct collocation method is used to enforce the essential boundary conditions.

3. Model and algorithm

The transient heat conduction equation (2D in this paper) for a stationary medium is given by [14]

$$\rho c_p \frac{\partial T}{\partial t} = \frac{\partial}{\partial x}\left(k_x \frac{\partial T}{\partial x}\right) + \frac{\partial}{\partial y}\left(k_y \frac{\partial T}{\partial y}\right) + G \tag{6}$$

where ρ is the density of material, c_p is the specific heat, k_x and k_y are the thermal conductivities in the x- and y-directions, respectively, G is the heat generation per unit volume. The initial conditions and boundary conditions for this type of problem are:

$$T(x,y,0) = T_0 \quad \text{in } \Omega \tag{7}$$

$$T = T_b \quad \text{on } \Gamma_b \tag{8}$$

$$k_x \frac{\partial T}{\partial x} n_x + k_y \frac{\partial T}{\partial y} n_y + q + h(T - T_a) = 0 \quad \text{on } \Gamma_q \tag{9}$$

where $\Gamma_b \cup \Gamma_q = \Gamma$ and $\Gamma_b \cap \Gamma_q = 0$ represent the whole boundary. In the above equations, n_x and n_y are direction cosines, h is the heat transfer coefficient, T_a is the atmospheric temperature and q is the boundary heat flux.

Before dealing with the temporal discretization, we use the standard Galerkin method for the transient equations. The temperature is discretized over space as follows:

$$T(x,y,t) = \sum_{i=1}^{n} N_i(x,y) T_i(t) \tag{10}$$

where N_i are the shape functions and $T_i(t)$ are the time-dependent nodal temperatures.

The Galerkin representation of Eq. (6) is

$$\int_{\Omega} N_i \left[\frac{\partial}{\partial x}\left(k_x \frac{\partial T}{\partial x}\right) + \frac{\partial}{\partial y}\left(k_y \frac{\partial T}{\partial y}\right) + G - \rho c_p \frac{\partial T}{\partial t}\right] d\Omega = 0 \tag{11}$$

Employing integration by parts on the first two terms of Eq. (11), we get

$$-\int_{\Omega}\left[k_x\frac{\partial N_i}{\partial x}\frac{\partial T}{\partial x}+k_y\frac{\partial N_i}{\partial y}\frac{\partial T}{\partial y}-N_iG+N_i\rho c_p\frac{\partial T}{\partial t}\right]d\Omega + \int_{\Gamma_q}N_i\left[k_x\frac{\partial T}{\partial x}n_x+k_y\frac{\partial T}{\partial y}n_y\right]d\Gamma_q=0 \quad (12)$$

Substituting Eqs. (9) and (10) into Eq. (12), we can obtain following equation:

$$-\int_{\Omega}\left[k_x\frac{\partial N_i}{\partial x}\frac{\partial N_j}{\partial x}+k_y\frac{\partial N_i}{\partial y}\frac{\partial N_j}{\partial y}\right]d\Omega T_j(t)-\int_{\Omega}\rho c_pN_iN_j\,d\Omega\frac{\partial T_j}{\partial t} + \int_{\Omega}N_iG\,d\Omega-\int_{\Gamma_q}N_iq\,d\Gamma_q-\int_{\Gamma_q}N_ih(T-T_a)\,d\Gamma_q=0 \quad (13)$$

where i and j represent the nodes. Eq. (13) can be written in a more convenient form as:

$$\boldsymbol{M}\frac{\partial\boldsymbol{T}}{\partial t}+\boldsymbol{KT}=\boldsymbol{f} \quad (14)$$

where

$$M_{ij}=\int_{\Omega}\rho c_pN_iN_j\,d\Omega \quad (15)$$

$$K_{ij}=\int_{\Omega}\left[k_x\frac{\partial N_i}{\partial x}\frac{\partial N_j}{\partial x}+k_y\frac{\partial N_i}{\partial y}\frac{\partial N_j}{\partial y}\right]d\Omega+\int_{\Gamma}hN_iN_j\,d\Gamma \quad (16)$$

$$f_i=\int_{\Omega}N_iG\,d\Omega-\int_{\Gamma_q}N_iq\,d\Gamma_q+\int_{\Gamma_q}N_ihT_a\,d\Gamma_q \quad (17)$$

If k_x and k_y are independent of temperature, Eq. (14) is linear in form, or Eq. (14) is non-linear and requires an iterative solution.

As can be seen from the semi-discrete form of Eq. (14), the differential operator involving the time-dependent term still remains to be discretized. In this paper, we use forward different technique for the time approximation, and then Eq. (14) can be written as:

$$\boldsymbol{M}\frac{\boldsymbol{T}^{n+1}-\boldsymbol{T}^{n}}{\Delta t}=\boldsymbol{KT}^{n}+\boldsymbol{f}^{\,n} \quad (18)$$

As mentioned above, the computational cost of EFGM is usually higher than that of FEM, especially for transient problems. Beside calculation of shape functions and its derivatives, the linear equations need to be solved in each time step, which requires more computational time than that of FEM. In order to avoid solving linear equations, we can use the mass lumping technique, that is, these mass matrices $\boldsymbol{M}$ can be "lumped" by summing up the rows and placing on the diagonals as in FEM, thus we obtain a matrix free formulation. This is an approximation, but a worthwhile and time-saving approximation. Mass lumping will eliminate the need for the matrix solution procedure necessary for consistent matrices. Moreover, the essential boundary conditions can be enforced straightforwardly as in FEM. As a matter of fact, mass lumping technique is used in FEM popularly, but not used in meshless method so far.

In order to evaluate the integrals in Eqs. (15)–(17), the problem domain is discretized into a set of background cells, and then the Gauss quadrature scheme is employed to perform the integrations numerically over these cells. In the paper, 3 × 3 Gauss points are used in each cell for numerical quadratures. In order to save computational time as much as possible, we can calculate shape functions and its derivatives only one time at the preprocessing stage if the nodes are unchanged during the analysis. Therefore, if the nodes are fixed during the calculation, the flowchart of EFGM for the transient heat transfer problems can be summarized as

1. *Preprocessing stage:*
- Define EFGM nodes and their initial position and temperature.
- Compute shape functions and their derivatives:
  – Loop over cells of the domain
    * Loop over quadrature points $\boldsymbol{x}_Q$ in cell C
    (a). if quadrature point $\boldsymbol{x}_Q$ is outside the physical domain, go to (d);
    (b). check all nodes in cell and surrounding cells to determine n nodes $\boldsymbol{x}_I$, I = 1 to n such that $\boldsymbol{x}_Q$ is in their domain of influence;
    (c). for each of the n neighbor nodes, compute $\boldsymbol{N}I(\boldsymbol{x}_Q)$ and its spatial derivatives;
    (d). continue;
    * End quadrature point loop
  – End cell loop
- Compute mass matrix $\boldsymbol{M}$ and then lump mass matrix, invert and store it in an array

2. *Computational stage:*
- Loop over time steps
  – Compute matrix $\boldsymbol{K}$ and $\boldsymbol{f}$ at each quadrature point
  – Impose essential boundary directly
  – Update T
- End loop over until reach the steady state or the given time steps

4. Results of numerical example and discussion

In this section, EFGM is applied to compute two-dimensional unsteady state heat conduction problem. Considering the square plate of unit size, three sides of the plate are maintained at the constant temperature 100 °C, and the upper side is subjected to 500 °C. The thermal conductivity of the material is constant and equal to 10 W/m °C [14].

The analytical solution to this problem for steady state is given by [15]

$$T(x,y)=(T_{top}-T_{side})\frac{2}{\pi}\sum_{n=1}^{\infty}\frac{(-1)^n+1}{n}\sin\left(\frac{n\pi x}{W}\right)\frac{\sinh\left(\frac{n\pi y}{W}\right)}{\sinh\left(\frac{n\pi H}{W}\right)}+T_{side} \quad (19)$$

where W is the width, H is the height of the plate, T_{top} is the temperature at the top side and T_{side} is the temperature at the other sides of the plate. Therefore, $T(0.5, 0.5) = 200$ °C.

Two different nodal distributions shown in Fig. 1(a) and (b) are used for the square plate problem to examine the efficiency of the present method. Additionally, Fig. 1(c) presents the finite element mesh. In the paper, linear triangular elements are used for FEM. In order to illustrate the computational accuracy of the present method, the results are compared between EFGM and FEM.

Figs. 2 and 3 show the temperature contours at t = 0.01 s and t = 0.5 s, respectively. In these figures, (a), (b) and (c) represent EFGM solutions for 1681 regularly distributed nodes, EFGM solutions for 2362 irregularly distributed nodes and FEM solutions, respectively. It can be noted that the results obtained by EFGM are identical with FEM solutions. Consequently, the mass lumping technique can be applied to EFGM. Moreover, the temperature reaches steady state about t = 0.5 s and a steady value at the centre of plate is (a) 199.98 °C, (b) 200.05 °C, and (c) 200.30 °C, respectively. We have known that under the steady state the analytical solution of that is 200 °C. Thus it indicates that EFGM coupling with mass lumping technique has high computational accuracy, especially for regular nodal distribution in this problem.

Fig. 4 presents the comparison of the temperature variation at the centre point (0.5, 0.5) of plate with respect to time, which is between the solutions of EFGM for two different nodal distributions,

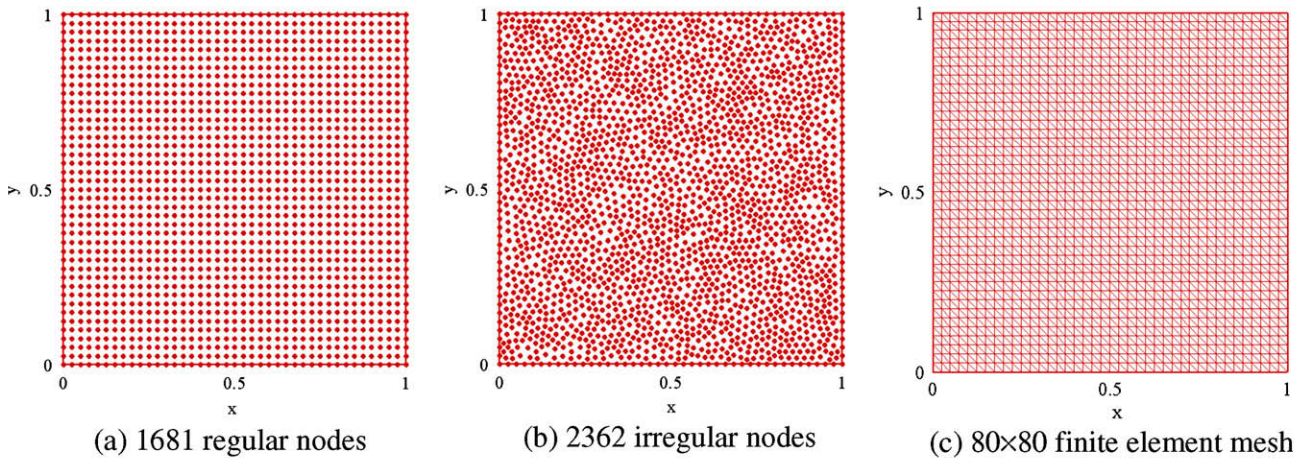

Fig. 1. Different nodal distributions used for EFGM and finite element mesh.

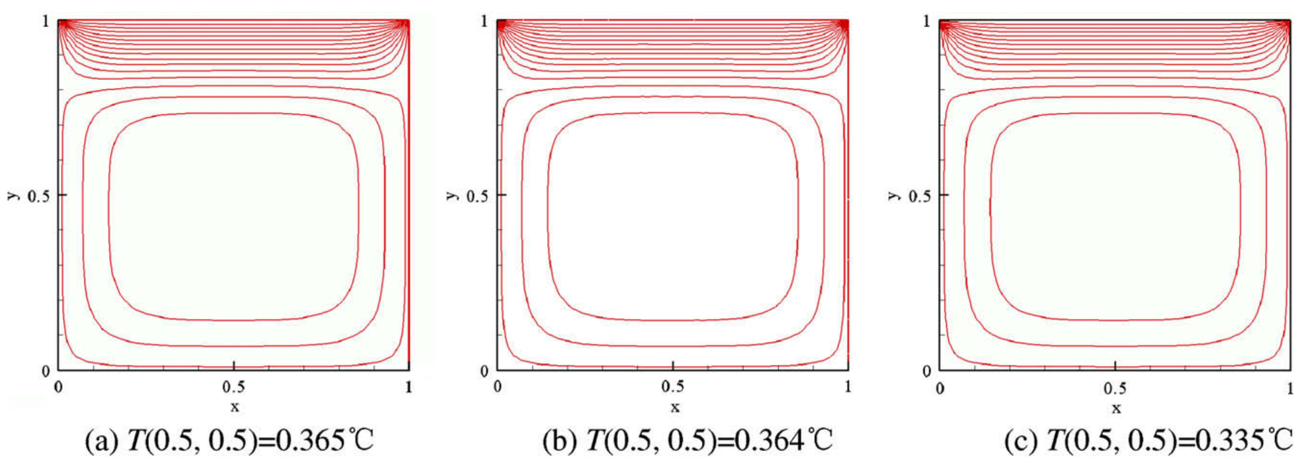

Fig. 2. Temperature distribution at t = 0.01 s for EFGM (a and b) and FEM (c).

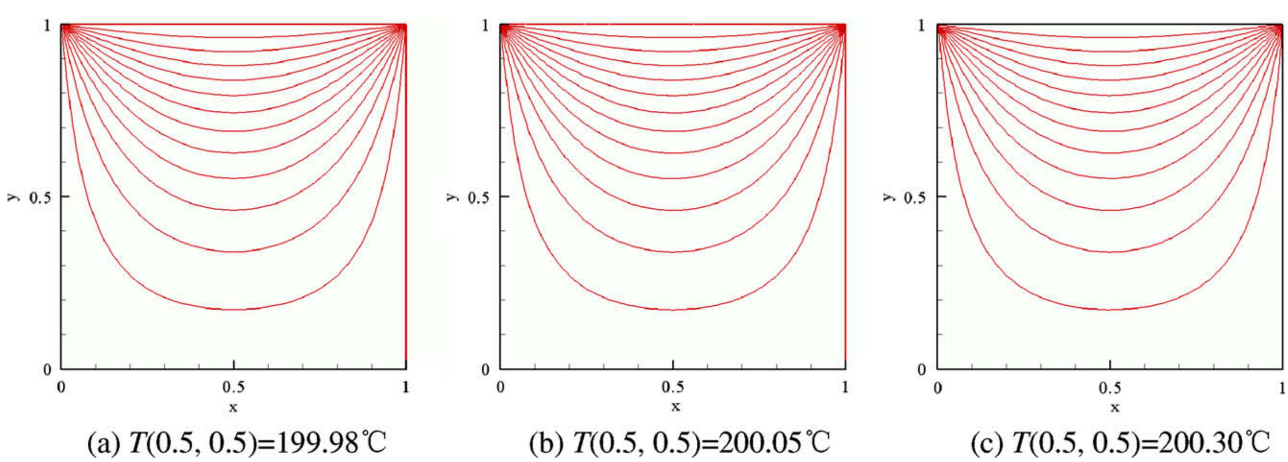

Fig. 3. Temperature distribution at t = 0.5 s for EFGM (a and b) and FEM (c).

namely regular and irregular nodal distributions, as well as between the solutions of EFGM for regular nodal distributions and those of FEM, respectively. It can be seen that these results are identical. It should be noted that the temperature increases rapidly and reaches a steady value about 0.4 s and thereafter remains constant.

To further demonstrate the advantages of EFGM combining mass lumping technique over the EFGM with consistence mass matrix in efficiency, all the computational parameters are identical. In the paper the time step Δt = 0.0001 s and the dimension of the influence domain for each node is assumed to be 1.3d, where $d = \sqrt{(\Delta x)^2 + (\Delta y)^2}$, Δx and Δy are nodal spacings in the x- and y-directions. Table 1 gives the comparisons of CPU times spent for running the example till t = 1.0 s by using EFGM and FEM with/without mass lumping technique. It can be seen that the present method accelerates computational efficiency evidently.

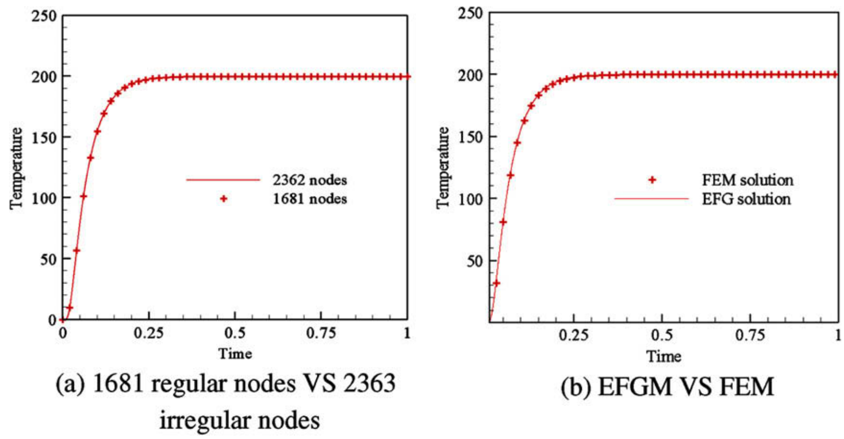

Fig. 4. Comparison of temperature distribution between EFGM solutions and FEM solution at the centre of a square domain with respect to time.

Table 1
Comparison of CPU time obtained by EFGM and FEM with/without mass lumping technique.

Techniques	CPU time (s)
EFGM with mass lumping	177.17
EFGM without mass lumping	1143.42
FEM with mass lumping	24.63
FEM without mass lumping	436.33

5. Conclusions

In the paper, EFGM has been successfully applied to the transient heat transfer problems. In order to reduce the computational cost of EFGM and simplify the solution procedure, the mass lumping technique is used. The numerical results obtained by the present method are compared with those obtained by FEM as well as analytical solutions, which indicates that: (1) The EFGM combining mass lumping technique provides a very efficient, fast and accurate method to solve transient heat transfer problems. (2) In general, the MLS shape functions do not satisfy the Kronecker delta condition, thus EFGM poses some difficulties in the imposition of essential boundary conditions. However, in the present method, once the mass matrix has been lumped, the essential boundary condition can be easily enforced as same as FEM's.

Acknowledgments

The support from the National Natural Science Foundation of China (NSFC) (No. 10590353) and National Basic Research Program of China (No. 2005CB321704) are fully acknowledged.

References

[1] T. Belytschko, Y. Krongauz, D. Organ, M. Fleming, P. Krysl, Meshless method: an overview and recent developments, Comput. Methods Appl. Mech. Eng. 139 (1996) 3–47.
[2] G.R. Liu, Y.T. Gu, An Introduction to Meshfree Methods and Their Programming, Springer, The Netherlands, 2005.
[3] I.V. Singh, A numerical solution of composite heat transfer problems using meshless method, Int. J. Heat Mass Transfer 47 (2004) 2123–2138.
[4] I.V. Singh, M. Tanaka, Heat transfer analysis of composite slabs using meshless element free Galerkin method, Comput. Mech. 38 (2006) 521–532.
[5] A. Singh, I.V. Singh, R. Prakash, Meshless analysis of unsteady-state heat transfer in semi-infinite solid with temperature-dependent thermal conductivity, Int. J. Heat Mass Transfer 33 (2006) 231–239.
[6] A. Singh, I.V. Singh, R. Prakash, Meshless element free Galerkin method for unsteady nonlinear heat transfer problems, Int. J. Heat Mass Transfer 50 (2007) 1212–1219.
[7] L.H. Liu, Meshless method for radiation heat transfer in graded index medium, Int. J. Heat Mass Transfer 49 (2006) 219–229.
[8] H. Wang, Q.H. Qin, Y.L. Kang, A meshless model for transient heat conduction in functionally graded materials, Comput. Mech. 38 (2006) 51–60.
[9] V. Sladek, J. Sladek, M. Tanaka, C.H. Zhang, Transient heat conduction in anisotropic and functionally grade media by local integral equations, Eng. Anal. Bound. Elem. 29 (2005) 1047–1065.
[10] J. Sladek, V. Sladek, C. Hellmich, J. Eberhardsteiner, Heat conduction analysis of 3-D axisymmetric and anisotropic FGM bodies by meshless local Petrov–Galerkin method, Comput. Mech. 39 (2007) 323–333.
[11] X.H. Zhang, J. Ouyang, Meshless analysis of heat transfer due to viscous dissipation in polymer flow, Eng. Anal. Bound. Elem. 32 (2008) 41–51.
[12] X.H. Wu, W.Q. Tao, Meshless method based on the local weak-forms for steady-state heat conduction problems, Int. J. Heat Mass Transfer 51 (2008) 3103–3112.
[13] M.Y. Zhang, H. Zhang, L.L. Zheng, Simulation of droplet spreading, splashing and solidification using smoothed particle hydrodynamics method, Int. J. Heat Mass Transfer 51 (2008) 3410–3419.
[14] R.W Lewis, P. Nithiarasu, K.N Seetharamu, Fundamentals of the Finite Element Method for Heat and Fluid Flow, Wiley, Chichester, 2004.
[15] J.P. Holman, Heat Transfer, ninth ed., McGraw-Hill, Singapore, 2002.